

**An Investigation of the Relationship Between Fracture Type and Force: Blunt Force
Trauma on Mammalian Juvenile Ribs (*Sus scrofa*, Linneaus)**

By

Katie A. Boyd

Submitted in partial fulfilment of the course

FORS 4095E

Department of Forensic Science

Laurentian University

Sudbury, Ontario

P3E 2C6

© Katie A. Boyd, 2017

ABSTRACT

The interpretation of bone trauma is an important aspect in understanding the circumstances within a death investigation (1-3). Proper interpretation of fractures can aid in identifying the number of blows, impact sites, the order in which they occur and the amount of force required to inflict such wounds (1,2). Yet there is a paucity of research regarding the force applied through the utilization of blunt implements used to inflict trauma. Such a study has the potential of more accurately characterizing the trauma, with regard to the amount of force used to create observed fracture patterns. In this preliminary study, a computer controlled impacting machine was used to inflict direct trauma onto several full, semi-fleshed racks of juvenile pig ribs (*Sus scrofa*, Linneaus) with a hammerhead attachment (n=36). Although there has been a recent interest in fracturing devices (2, 4-6), this one differs in that it mimics the arching motion of a human overhand swing, and is able to inflict trauma onto fully fleshed and intact specimens. After each strike the force at the moment of impact was recorded and was later paired with its corresponding fracture. From there, the range of force associated with transverse, oblique, spiral, greenstick, and comminuted fractures, as well as having no fractures at all were examined in light of the recorded forces. Such results were compared to those of others performed prior to work on the machine to determine if such relationships were consistent between studies. In this study it was discovered that there is no threshold where one fracture group will start and another will end.

KEYWORDS

Forensic Science, Forensic Anthropology, Blunt Force Trauma, Fracture, Force

ACKNOWLEDGEMENTS

The first group of individuals whom I gratefully acknowledge are Alexandra DeMarco, Henna Ali, and Rebecca Louwagie, the darling souls I was pleased to call my roommates during the last year of my undergrad. This also extends to the lovely Rebecca Chapman, whose love was radiated from 5 hours away. Without your words of encouragement and praise, and the couple hundred revisions, this thesis document would have never taken shape. I am blessed to have such a great group of individuals in my life.

I would also like to acknowledge my loving parents, Lisa and John, who have never for a second doubted me or my dreams. Whom have shaped me into the individual I am today and always pushed me to do better for myself.

Many thanks also go out to those of the faculty members at Laurentian University, especially Tracy Oost, whom have generously donated some of their time and expertise to me when I was in what looked to be desperate need. And Bailey Henwood, thanks for being my thesis buddy!

Finally, I extend my deepest of thanks to my thesis supervisor, Dr. Scott I Fairgrieve, for providing me with the experience of a life time. If I could go back and do it all again, I wouldn't change a thing!

TABLE OF CONTENTS

ABSTRACT	2
ACKNOWLEDGEMENTS	3
LIST OF TABLES	5
LIST OF FIGURES	6
CHAPTER 1: INTRODUCTION AND BACKGROUND.....	8
1.1 Introduction and Statement of Problem	8
1.2 General Background	9
1.2.1 Blunt Force Trauma.....	9
1.2.2 Mammalian Bone Structure and Tissue Types.....	10
1.2.3 Factors Influencing Fracture in Blunt Force Trauma	13
1.3 Fracture Type and Blunt Force Trauma.....	15
1.4 <i>Sus scrofa</i> (Linneaus) as a Human Analogue	20
1.5 Research Goals and Objectives.....	21
CHAPTER 2: MATERIALS AND METHODS	22
2.1 Sample Preparation	22
2.2 The Traumatizer.....	23
2.3 Trauma Infliction	27
2.4 Maceration and Macroscopic Analysis.....	29
CHAPTER 3: RESULTS	31
3.1 Fracture Types	31
3.2 Force Determination	33
3.3 Fracture and Force Association	34
3.4 Statistical Analysis.....	36
CHAPTER 4: DISCUSSION	38
CHAPTER 5: CONCLUSIONS	43
5.1 Conclusions.....	43
5.2 Limitations and Future Research	43
APPENDIX I	44
REFERENCES.....	47

LIST OF TABLES

3.1	Fractures observed after impact and their associated ranges of force.....	34
3.2	Table representing the results from multiple Mann-Whitney U tests.....	36
4.1	Table comparing the different fractures seen between this study, and the study by C.Holinier.....	37
4.2	Fractures observed after impact and their associated ranges of force of C.Holinier's study.....	39

LIST OF FIGURES

1.1	Graph Representing the Relationship Between Stress and Strain, or, Young's Modulus (as proposed by Love & Symes, 2004).....	13
1.2	The Five Different Forces That Result in Fracture (as proposed by Galloway <i>et al</i> , 1999).....	14
1.3	Complete Fractures of Bone (as proposed by Galloway, 1999).....	16
1.4	Incomplete Fractures of Bone (as proposed by Galloway, 1999).....	17
1.5	Fractures that are most often observed on the thoracic cage (as proposed by Galloway, 1999)	19
2.1	Full left rack of juvenile porcine ribs (Photo by K.A. Boyd)	21
2.2	The Traumatizing unit (Photo by K.A. Boyd)	22
2.3	The hammerhead attachment (Photo by K.A. Boyd)	23
2.4	The piston system that operates the impacting arm (Photo by K.A. Boyd).....	24
2.5	The pressure gage that must be read between 140 and 160psi (Photo by K.A. Boyd).....	25
2.6	Full left porcine rib rack split into upper and lower halves (photo by K.A. Boyd).....	26
2.7	Half of a porcine rack suspended in the impacting hub (Photo by K.A. Boyd).....	28
3.1	1LUR2 exhibiting a transverse fracture (Photo by K.A. Boyd).....	30
3.2	2LLR11 exhibiting an oblique fracture (Photo by K.A. Boyd).....	30
3.3	1LUR6 exhibiting a spiral fracture (Photo by K.A. Boyd).....	31
3.4	3LUR2 exhibiting a comminuted fracture (Photo by K.A. Boyd).....	31
3.5a	2RLR3 exhibiting a greenstick fracture (Photo by K.A. Boyd).....	31
3.5b	2RLR3 exhibiting a greenstick fracture (Photo by K.A. Boyd).....	32
3.6	2RUR5 exhibiting no fracture (Photo by K.A. Boyd).....	32
3.7	Graph generated by the impacting computer system for the force applied throughout the trial.....	33
3.8	Box and whisker plot displaying the overlap between forces applied and their associated fracture types.....	34
4.1	Graph generated by the impacting computer system for the force applied throughout the trial of C.Holinier's study.....	38
4.2	Box and whisker plot displaying the overlap between forces applied and their associated fracture types of C.Holinier's study.....	40

4.3	Graph representing the median distribution of the fracture types and their associated forces.....	41
4.4	Graph representing the median distribution of the fracture types and their associated forces of C.Holinier's study.....	41

CHAPTER 1: INTRODUCTION AND BACKGROUND

1.1 Introduction and Statement of Problem

The interpretation of bone trauma is an important aspect in deciphering the circumstances surrounding a death investigation (1,2). Forensically, establishing proper wound discernment may assist in the re-construction (2,7) of dynamic perimortem events (8), as well as aid in the identification of the perpetrator and the weapon(s) used (1,2,8). Since not much is known about the extent of the events surrounding a death investigation, reliable reconstruction is unavailable (3). This can become extremely difficult in the absence of soft tissue, and such interpretations require an advanced understanding about specific bones and the way they fracture (2,4,9). In medicolegal death investigations, forensic experts such as anthropologists and pathologists, use their extensive knowledge in skeletal trauma in courtroom settings to answer questions regarding the cause and manner of death (3), the number of blows, impact sites, and the order in which they occur (2). They may also be asked questions regarding whether the induced trauma was accidental or intentional (2), which would require the expert to comment about the amount of force needed to show such patterns (2,7). This is a topic that is very scarcely researched within the literature, especially when it comes to the skeletal elements of the thoracic cavity (3).

The way the human chest responds to blunt force trauma is a focus of many research domains such as those including suicides, falls, child abuse, and road traffic accidents (2,5,8). Many recent experiments have been exploring the use of machines to predict the behaviours of bone under force (2,4-6), yet the way ribs fracture under blunt traumatic loads is poorly understood (6). To improve the understanding of chest injuries a better knowledge of rib response to dynamic forces is needed (5), and such responses have received very little attention in anthropological literature (9), however, recent studies have begun to show an interest in such.

It is predicted that this is because, even though the ribcage does play an important role in respiration, protection, and support, it is not of immediate medical attention (9). Even when the ribs are fractured intercostal muscles maintain the architecture of the pleural cavity and prevent consequential injuries to the underlying organs (10). This study aims to quantify the relationship between force and fracture type.

1.2 General Background

1.2.1 Blunt Force Trauma

Trauma refers to a sudden physical injury obtained by violence or an accident (1). It is a mechanism that is related directly to the force, or the combination of forces that may produce alterations to the skeleton (3). These forces can be divided into three main categories; sharp force, ballistic (high-velocity), and blunt force trauma (1,8). Sharp force trauma, as its name indicates, is an injury that is directed along a narrow surface by an object with a point or an edge. (8,11). The forces associated with sharp force trauma are those of puncturing, cutting, chopping, sawing, or crushing (11). Ballistic trauma is defined as being relatively high velocity impacts dispersed over relatively small surface areas, and can be evident in cases involving firearms (8). The last of the three is blunt force trauma. This is defined as being relatively low velocities over a relatively large surface area (8). Due to the complexities and uniqueness of each of these types of fractures, blunt force trauma will be the sole focus of this study.

Blunt force trauma may cause injuries to both the hard and soft tissues of the body. Skeletal elements could be fractured, and superficial elements could be bruised, abraded, or lacerated (12). The fracturing of skeletal elements can be caused either through direct contact of the thoracic cage, or through indirect contact by the dynamic forces that pull, twist, or rotate the bone (8). Such variations in forces can result in any number of different fractures that depend on

the instruments used (1). For example, it has been found that homicides associated with blunt force trauma utilizing sticks, clubs, or even fists are not uncommon (1,8). In addition, any number of hard surfaces can inflict blunt force trauma as well, such as steering wheels, or rocks on the ground during a fall (1). Due to the varying nature of blunt force trauma, it is probably the most complex and challenging for forensic anthropologists to assess as the patterns seen are far from being classic (3).

Trying to assess the circumstances surrounding the death through analysis of blunt force trauma to the skeleton and in absence of any other dependent data is not as clear-cut as cases involving sharp or ballistic trauma (1,3). Homicide scenes can often include a lot of movement (8), and can result in many different forces being applied to the rib cage. This in turn can result in different fractures depending on the instrument being used (1). The following sections discuss the factors that influence fractures in cases of blunt force trauma.

1.2.2 Mammalian Bone Structure and Tissue Types

Bone is a strong and light weight connective tissue that is made up of a mineralized protein network of hydroxyapatite ($\text{Ca}_{10}(\text{PO}_4)_6(\text{OH})_2$) and collagen (8,9) that houses blood, water, amorphous polysaccharides, cells, and blood vessels (8,13). Bone is made up of two different types, cortical and cancellous (13-16). These layers are identical at the molecular and cellular levels, and only differ when it comes to their overall structure (14). Cortical bone consists of the dense exterior surface for muscle attachment (13,15), and provides the tissue with strength and rigidity. Cancellous bone (often referred to spongy or trabecular) is deep to the cortical bone, and is primarily found in the ends of long bones, the interior of cuboidal and flat bones, and between the layers of cortical bone in the skull (13). It is composed of interlamellar

sheets of crystallized collagen fibres that are honeycombed together. This creates air pockets within the bone to keep it light weight, and constrains fracturing as it allows for a sudden force to disperse (9). In rib bones the hard, outer compact surface is very narrow while the center cavity of spongy bone is large and porous.

Both categories of bone are composed of two types, woven and lamellar (13,15). Woven bone consists of randomly orientated collagen fibers that weave through blood vessels and nerves (13). Lamellar bone has a much more organized structure that is slowly produced as an individual ages (13). It consists of parallel layers of collagen fibers called “lamellae” (13).

1.2.2.1 Aging of Bone

Bone is a highly vascularized connective tissue that is constantly changing (14). In ribs, bones form out of a random network of hyaline cartilage matrix, a phenomenon called endochondral ossification (14). This bone tissue can be seen as early as the eighth week of gestation through the formation of ossification (bone creating) centers (14). This is a very slow process that continues after birth, thus the bones of juveniles consist mostly of a very elastic and compressible cartilage that is very dense and strong (8,9,14). Over time, the cartilage will begin to be replaced by bone with the help of calcium (ossification) from the inside, out (14).

In the early stages of bone life, vascularization and nutrient waste exchange centers within the cortical bone are surrounded by structures called primary osteons. (9,13,14). These osteons have a very limited life span, and are later replaced by secondary osteons (13). This phenomenon is known as bone remodeling and happens when the body displays hormonal changes or there need for calcium (8). It is constantly ongoing throughout our lives, and allows for the renewal of bone tissue as well as accommodates for change in bone architecture (8). A

combination of osteoclasts and osteoblasts break down and remodel the bone into a secondary structure (8). This secondary bone is also referred to as Haversian bone and contains structures called Haversian systems consisting of a Haversian canal surrounded by several layers of lamella that contains blood vessels and nerves (14,15). Secondary osteons can be distinguished from those of primary through the visualization of cement lines (13). These are structures that envelop secondary osteons, and intersect older (either primary or secondary) lamellae that are circular in shape resulting in interstitial lamellae (13).

Each time the bone is remodeled, it increases the chances of fracture when a stress is applied. Remodeling increases the amount of minerals in the bone, reducing its flexibility (8). Haemopoatic tissue is replaced with fatty tissue that is less able to absorb energy (9), and the presence of cement lines give a more direct pathway for fracture proliferation (9). In turn, adult ribs may fracture under less force than those of juvenile ribs.

1.2.2.2 Anatomy of a Rib Bone

The ribs are a semi-elastic bone that wraps around the thoracic cavity. In adult humans, there are 12 ribs on each side, however this number is variable (18). The upper seven ribs (numbers 1-7) are known as true ribs and articulate directly with both sides of the sternum via costal cartilages. Ribs 8, 9, and 10 are known as false ribs, and are connected medially by cartilage articulating with the sternum via their superior rib. The last two ribs, 11, and 12, are known as floating ribs and lack any costal cartilage connection. All ribs articulate with the thoracic vertebrae on their proximal ends. Because of the arching nature of the thorax (human or pig), each rib will display a curved structure that results in an arched shape of a rib. In adult humans, rib bones 1-7 increase in length and are less oblique than ribs 7-12, whose length decreases and are more oblique (14,18). Pig ribs follow this same pattern, although in this study

the porcine racks that were purchased were composed of up to 13 ribs, so the change in shape must be considered.

1.2.3 Factors Influencing Fracture in Blunt Force Trauma

1.2.3.1 Stress and Strain

To understand the circumstances in which a bone will fracture, the relationship between stress and strain should be clearly understood. Stress is defined as the pressure that is exerted on a material or an object. It is used to measure the force applied over the cross-sectional area in which it is applied in psi (pounds per square inch) (8). Strain is defined as being the deformation in the change in its shape (8). In the beginning, when a stressor is applied to a bone, there is a linear relationship in the way the bone is strained (Figure 1.1). If this stressor is removed before reaching a plateau point, or the “yield point,” the bone will undergo a process called elastic deformation. This is the temporary bending of the bonds between atoms, and the bone will readily return to its original state once the stressor is released (8,9). However, if the stressor is not lifted before this yield point, the bone will undergo a process referred to as “plastic deformation” or, the permanent bending of bonds between atoms within the bone (9), and may be visualized as a series of microfractures on the shaft (8). If this stress is further continued, the bone will reach its failure point, resulting in fracture (4).

The failure point of bone is not always caused by an acute stressor. Over time, as the bones of the body are repeatedly stressed, the composition of their overall structure begins to change. This chronic stress results in a more fragile bone that is easier to break. At this point, even the smallest of acute stressors, such as reaching, could cause the bone to fracture. Various diseases and dietary deficiencies may also affect the bone structure and increase the chances of fracturing (14).

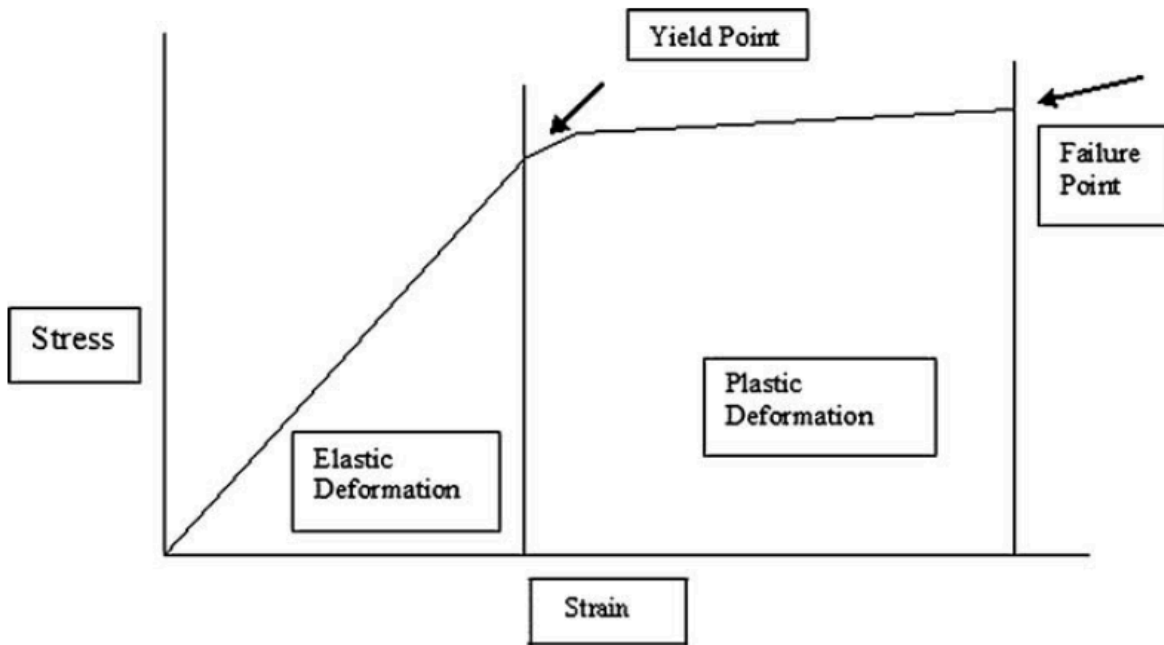


Figure 1.1 Graph Representing the Relationship Between Stress and Strain, or, Young's Modulus (as proposed by Love & Symes, 2004)

1.2.3.2 Force

The way bones respond to stress is dependent on the force that is applied (its amount, directionality, surface area, and loading rate), and the mechanical properties of the bone (density, composition, shape, collagen orientation and rigidity) (9). According to Galloway, there are five main forces that can result in the fracturing of skeletal elements. A summary of these forces is found in Figure 1.2. Compression occurs when the bone is subject to force squeezing the bone from opposite sides. Similarly, tension forces are of those that pull the bone ends apart. Rotational forces are caused when there is a twist in the axis of the bone. Shearing forces are parallel to one another that act on opposite sides of the bone and in opposite directions. Lastly,

bending forces are a combination of compression, tension, and shear forces. One side of the bone is being compressed, the other is being tensed, and a parallel force is applied in between.

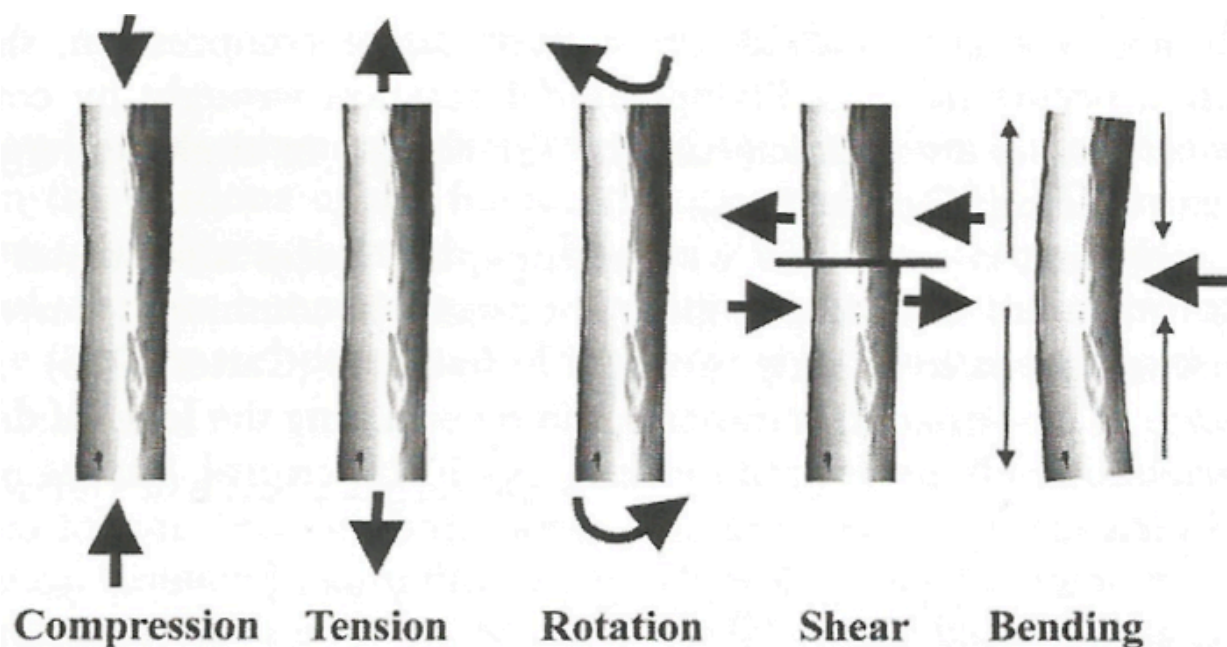


Figure 1.2 The Five Different Forces That Result in Fracture (as proposed by Galloway *et al*, 1999)

1.3 Fracture Type and Blunt Force Trauma

Fracture types of the skeletal elements are organized by their degree and overall pattern (8). The two main categories are those of complete and incomplete fractures. Complete fractures are defined as bearing an overall discontinuity between areas of the same bone (8). This group can be further subdivided into four categories; transverse, oblique, spiral, and comminuted.

Transverse fractures occur when the fracture line lies at a 90° angle to the long axis of the bone. In previous studies, these fractures have been seen to occur under high energy bending and tensional forces such as getting hit by a car or falls from great heights (2). *Oblique fractures*, very similar to transverse, have a fracture line that lies at an angle (approx. 45°) to the long axis

of the bone. These fractures are usually the result of a combination of rotational compressive and bending forces of moderate intensity (2). When the rotational force is the predominant force this will cause a long fracture line that covers a large surface area will result, however, if bending or compression forces are predominant the fracture line will be much smaller (2). *Spiral fractures* are similar to oblique fractures in that they are an angled fracture line that is twisted around the axis of the bone. The fracture lines of spiral fractures are sharp and pointed, and are generally more often seen in the weight-bearing bones of the body (such as the femur). They are caused by low-velocity rotational forces applied to the bone, or when there is a mixture of torsional and bending forces (2). One can tell the direction of the torsional forces by looking at the direction in which the spiral travels, and can be used to reconstruct the events surrounding the trauma (2). Finally, *comminuted fractures* happen at higher velocities of forces, and shatter the bone into multiple (3+) fragments (8) (see Figure 1.3). A specific name can be given to a comminuted fracture that shares many characteristics with an oblique fracture. It is called a butterfly fracture, and this occurs when a lower force range is applied (2). Butterfly fractures are wedge-shaped fractures where the initial fracture began as a transverse fracture (tension failure), and then split into two oblique fractures (tension failure) in opposite directions (2). Higher speeds and more dynamic forces will cause the bones to split into more pieces and cause a higher number of comminuted fractures which can be seen in the case of ballistic trauma.

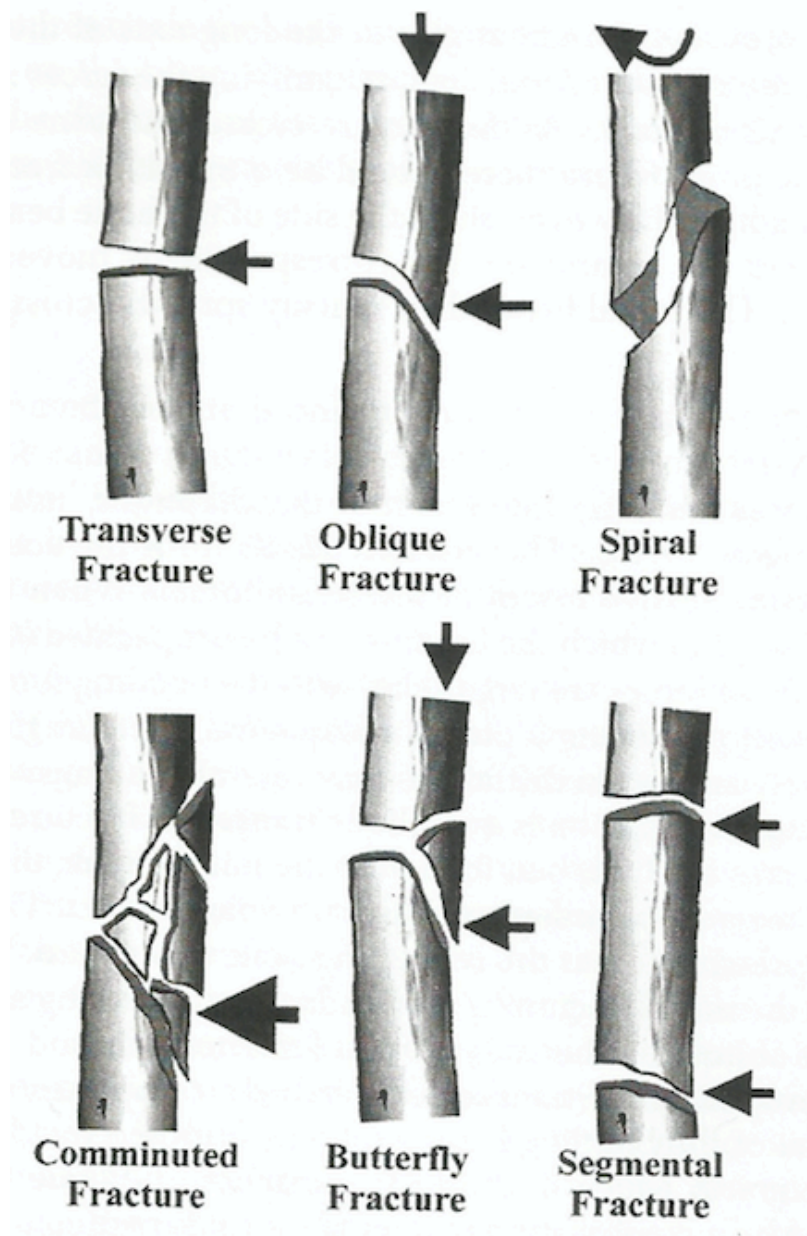


Figure 1.3 Complete Fractures of Bone (as proposed by Galloway, 1999)

Incomplete fractures are defined as being fracture lines that do not separate the bone into separate pieces. Instead, the fracture line only goes part way through the bone. There are three different incomplete fractures that may occur to the shafts of rib bones. The first is a bow fracture. This fracture is said to occur during the plastic deformation of the bone, and can be seen as multiple micro-fractures along the shaft of the bone. The second, a Torus fracture, or a Buckle

fracture, appears to be an incomplete transverse fracture, where the fracture line does not go through the entire shaft of the bone. The third is a greenstick fracture, which is very common in elastic juvenile bone when a stressor is acted upon one side of the bone, and the fracture lines accumulate on the opposite (8) (see Fig. 1.4). It was once argued the greenstick fractures only occurred in the elastic bones of juveniles but in one study, greenstick fractures to the rib cage were observed in individuals ranging between 21-76 years of age (9).

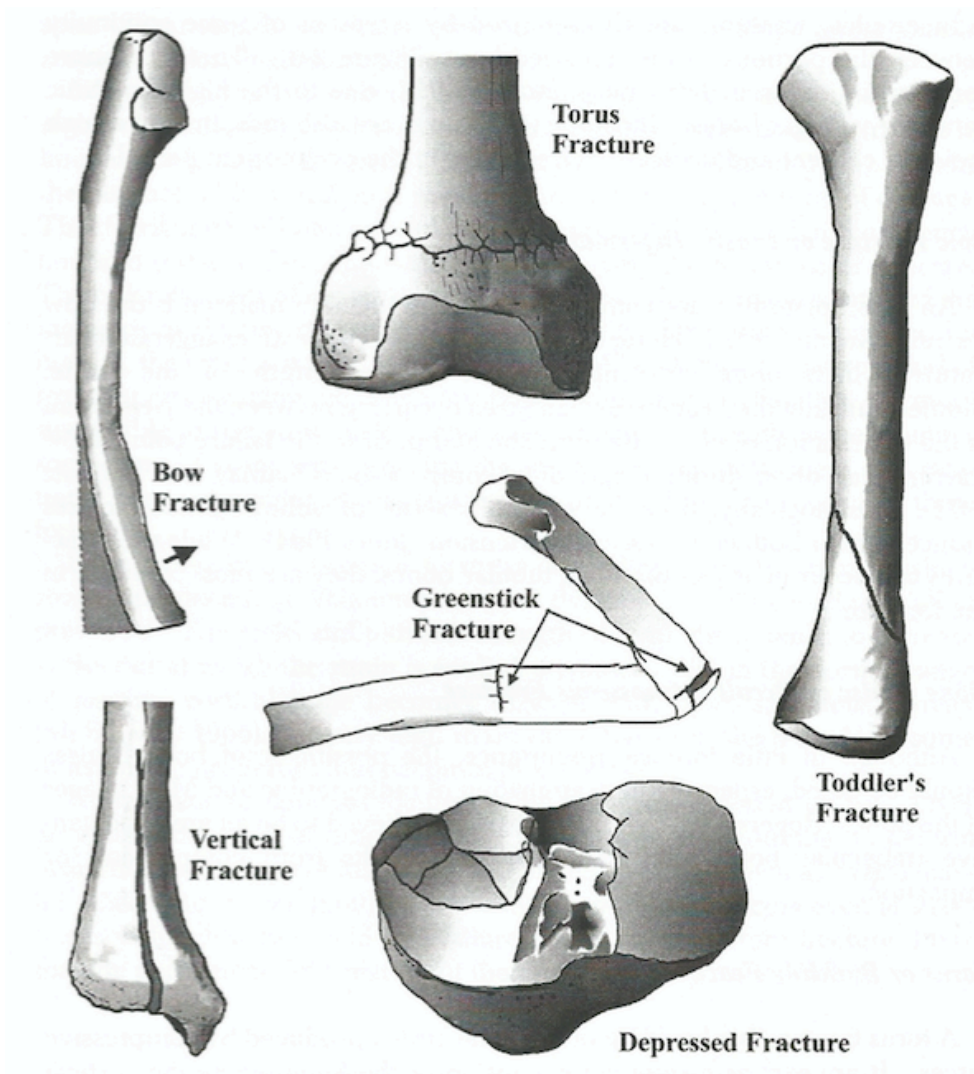


Figure 1.4 Incomplete Fractures of Bone (as proposed by Galloway, 1999)

Galloway (1999) notes that transverse and oblique fractures are the most common to occur on the thoracic cage with direct blows to the chest. However, Blout (1995, 1997) has argued that only greenstick fractures will occur on the ribs because of their elastic properties, especially those of juveniles (as cited by 8). A schematic showing the aforementioned fracture types commonly encountered on rib bones is in Figure 1.5. Some other experiments have found that ribs tend to fail under compression forces prior to tension, and that incomplete fractures can be seen in bones of the elderly (9). We can conclude from these studies that ribs respond unexpectedly to force. The ways in which they fracture depend upon nature of the force being applied and the biomechanical properties of the bone tissues. Because bone is a heterogeneous material, it complicates the prediction in the point of ultimate failure. Shape, strength, mineralization, and density of the bones, as well as the shape, mass, surface area and velocity of the instrument used all have an impact on the way a bone will fracture (8).

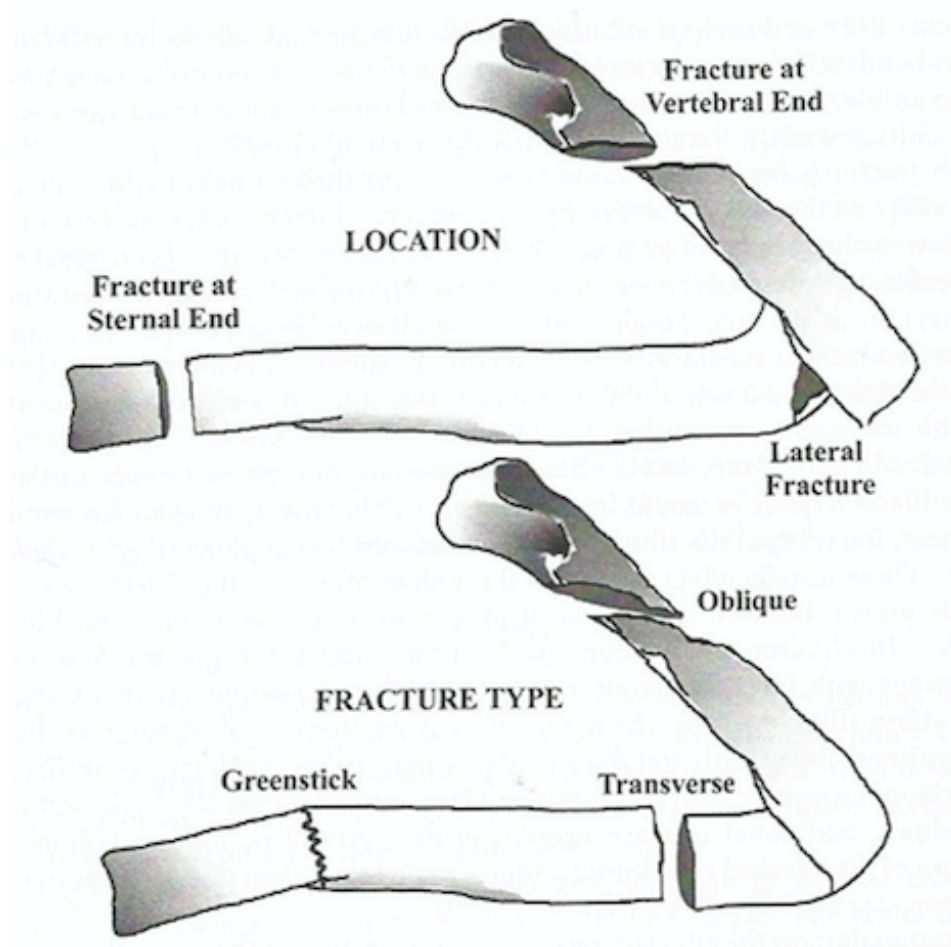


Figure 1.5 Fractures that are most often observed on the thoracic cage (as proposed by Galloway, 1999)

1.4 *Sus scrofa* (Linnaeus) as a Human Analogue

Although it would have been preferred to conduct this study with human rib samples, the ethics surrounding such research is very controversial. Animal models have been widely utilized as human analogues in forensic trauma interpretation (2,7,12,19-22). In this study, juvenile porcine ribs were chosen because they could be collected from a local butcher's shop with some soft tissue remaining and the periosteum still intact. It has also been noted that pig bones have very similar densities, shapes, and microstructures making them an excellent substitute for

human strength and mass (2,7,13). It is important to note, however, that the bones of immature pigs express more plexiform bone properties (a type of primary bone tissue), but is only characteristic in those of fast growing long bones of the animal (2). Overall, when Haversian bone tissue between humans and pigs (especially when fragmented) is examined microscopically, there are no gross diagnostic features that aid in distinguishing between species or anatomical origin (13).

1.5 Research Goals and Objectives

This study utilizes a computer-controlled impacting device to inflict blunt force trauma to juvenile porcine ribs using a modified hammerhead. This experiment has been conducted once before by C. Holinier (2016), and their results will try to be replicated.

Although hammers are not weapons often documented in homicide cases, it is obvious that with their wide-ranging availability they may be utilized to inflict harm upon others. They may be used in both impulsive killings where a hammer may be the first weapon at hand, or in premeditated homicides outside of the home (23). In such cases, perpetrators may choose light weight and easy to carry weapons that do not draw suspicious attention (23,24).

Currently, there is no such technique for interpreting injury mechanisms of blunt force trauma on the bones of the thoracic cage. Croft (2016) states that “the determination of the mechanism that results in particular patterns is better approached through experimentation rather than theorizing.” This study answers Croft’s call, as the objective of this study is to reveal the association between the energy of a force, and the associated fracture pattern.

CHAPTER 2: MATERIALS AND METHODS

2.1 Sample Preparation

As per regular practice in forensic science, semi-fleshed *Sus scrofa* (otherwise known as domestic pig) ribs were purchased from a local butcher's shop in Sudbury, Ontario. Upon purchasing, it was asked that the samples consist of side ribs with as little costal cartilage as possible. For this study, 4 porcine racks were purchased (three left and one right) each containing between 12 and 13 ribs (Figure 2.1). Three of the rib racks were purchased fresh and were traumatized hours later. These racks were labeled 1, 2, and 3, with each individual rib number designated R1, R2, R3, etc. The last rack was purchased frozen and left to defrost in a refrigerator (approximately 2°C) overnight (labeled rack 4). Thankfully, the biomechanical structure of bone is not jeopardized if a bone is completely thawed before experimentation (4,22).



Figure 2.1 Full left rack of juvenile porcine ribs (Photo by K.A. Boyd)

2.2 The Traumatizer

The Traumatizer was built by students of the Bharti School of Engineering under the supervision of Dr. Brent Lievers at Laurentian University in Sudbury Ontario, Canada (Figure 2.2). The machine is composed of a pivoting arm with an interchangeable head where different implements can be attached. In this study, a hammerhead with a 2.5cm diameter was used to strike juvenile porcine ribs (Figure 2.3).



Figure 2.2 The Traumatizing unit (Photo by K.A. Boyd)



Figure 2.3 The hammerhead attachment

The inspiration behind this impacting device was the arching motion of a human over-arm swing. The arm of this machine is controlled by a piston that expands when air pressure is forced into it. This piston is located underneath the arm of the machine (Figure 2.4), so that when air is being forced through the piston, it grows longer and raises the arm. This buildup of pressure in this cylinder can be changed by the rotation of a dial and will determine the speed in which the arm travels. The pressure is generated from a Porter Cable Brand 6 gal 150 psi portable air compressor, and should always be read on a gage to be between 140 and 160psi while running a test (Figure 2.5). When the pressure is released, the arm will fall.

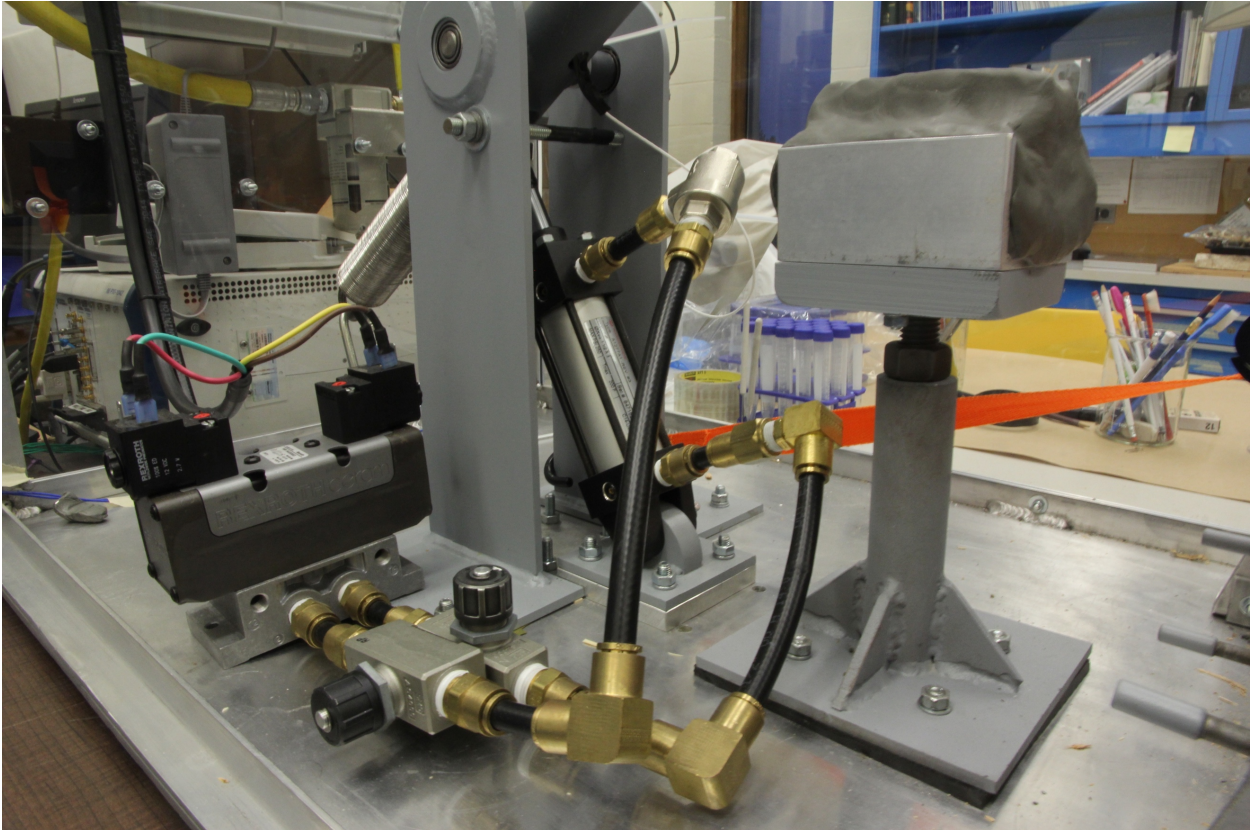


Figure 2.4 The piston system that operates the impacting arm (Photo by K.A. Boyd)



Figure 2.5 The pressure gage that must be read between 140 and 160psi (Photo by K.A. Boyd)

The impacting unit in its entirety is controlled by a computer software program that was designed specifically for this purpose. It has a built-in safety feature and will not run unless all the doors are locked shut. When a trial is run from the monitor, the software immediately begins to record the time. A load cell that is located at the end of the arm measures several variables during the run. It records the force (N), the vertical displacement (m) and the speed of the striking arm. From these variables, the machine can then calculate the acceleration (m/s^2) and velocity (m/s), through derivatives of these variables. Utilizing this information, the software creates graphical representations of each of these variables, plotting them against the time taken to run the trial. In this experiment, only the impact force graphs were analyzed.

2.3 Trauma Infliction

After inspection for pathology and any other damage that could have interfered with the experiment, each of the racks were cut between the seventh and eighth ribs, separating them into upper and lower halves. This allowed for the samples to fit more easily into the impacting machine (Figure 2.6). Upon unraveling the first rib samples it was discovered that the lower half of rack one (ribs 8-13) were purchased pre-fractured and therefore were not used in this study. The rest of the separated rib halves were wrapped in plastic wrap to keep the soft tissue intact during the traumatizing process.



Figure 2.6 Full left porcine rib rack split into upper and lower halves (photo by K.A. Boyd)

Before each rib was placed into the impacting hub, a series of trial runs of the machine were conducted to predict how much force the instrument would strike with. Because the arm

was controlled by compressed air, no runs back-to-back runs produced the exact same amount of force. Instead, they would produce forces that were a couple of hundred Newtons apart (refer to Appendix I). Once happy with the series of resultant forces run in practice, each rib half was positioned one-by-one onto the metal sheet inside the traumatizer unit. This metal sheet had an opening at the site of impact to allow for the suspension of long implements (such as in sharp force trauma), thus cardboard was placed underneath the samples to try to support the samples as best as possible without abruptly stopping the force of the arm. A clay slab was also positioned underneath the arm of the impacting machine to help stop the oscillation of the hammerhead after impacting.

Each rib was strapped down to the metal plate on either side of the rib to be struck so as to stop the hammerhead from moving the samples as best as possible (Figure 2.7). Each rib was subjected to a single blow, and successive blows were scattered to prevent further unwanted fracturing of a fracture formed in the previous trial, or in a rib that was yet to be traumatized. Each time a rib was struck, the time and date of the trial had been recorded so its associated force could be determined later.



Figure 2.7 Half of a porcine rack suspended in the impacting hub (Photo by K.A. Boyd)

2.4 Maceration and Macroscopic Analysis

Once all ribs in a subsample were struck by the instrument, each were separated from one another through the middle of the intercostal musculature and were grossly dissected with a scalpel. Each of the ribs subjected to trauma were individually placed inside a Ziploc bag labeled with the date, and their rack and individual rib number. These baggies were placed in a large storage freezer until later use. All un-impacted ribs were discarded.

When the samples were retrieved (approximately one month later), each bone was individually placed into a labeled beaker and was boiled on a hot plate for approximately one hour (103°C) making sure to keep track of what rib it was, and which rack it came from. This enabled most of the now off-white coloured flesh to peel off easily. To further clean the bones and remove any leftover stubborn material, the ribs were further boiled in a 3.5g/L Tergazyme[®]

detergent solution at approximately 97°C for one hour. This enabled the rest of the residue to be easily peeled away with the help of running water and a wooden popsicle stick. Wood was used because it is much softer than bone and when scraped against the bones surface it would not leave behind damage. When clean, the bones were placed onto a plastic tray covered in brown construction paper to dry. Each of the ribs was outlined and their date, rib number, and rack number were recorded.

After all the ribs were defleshed and dry, each was picked up one by one to analyze (1) if there was a fracture, and (2) what type of fracture it was. The samples were labeled as belonging to transverse, oblique, spiral, greenstick, comminuted (3+ pieces), or no fracture groups (Refer to Appendix I Table A).

CHAPTER 3: RESULTS

3.1 Fracture Types

A total of 36 rib samples were subjected to direct blunt force trauma in this study. A total of 19 transverse fractures, 4 oblique fractures, 3 greenstick fractures, 2 spiral fractures, and 3 comminuted fractures were observed (Figures 3.1 to 3.5). There were also instances where a force was applied and resulted in no fracture. This happened 5 times, and a resultant picture can be seen in Figure 3.6.



Figure 3.1 1LUR2 exhibiting a transverse fracture (Photo by K.A. Boyd)



Figure 3.2 1LLR11 exhibiting an oblique fracture (Photo by K.A. Boyd)



Figure 3.3 1LUR6 exhibiting a spiral fracture (Photo by K.A. Boyd)



Figure 3.4 3LUR2 exhibiting a comminuted fracture (Photo by K.A. Boyd)

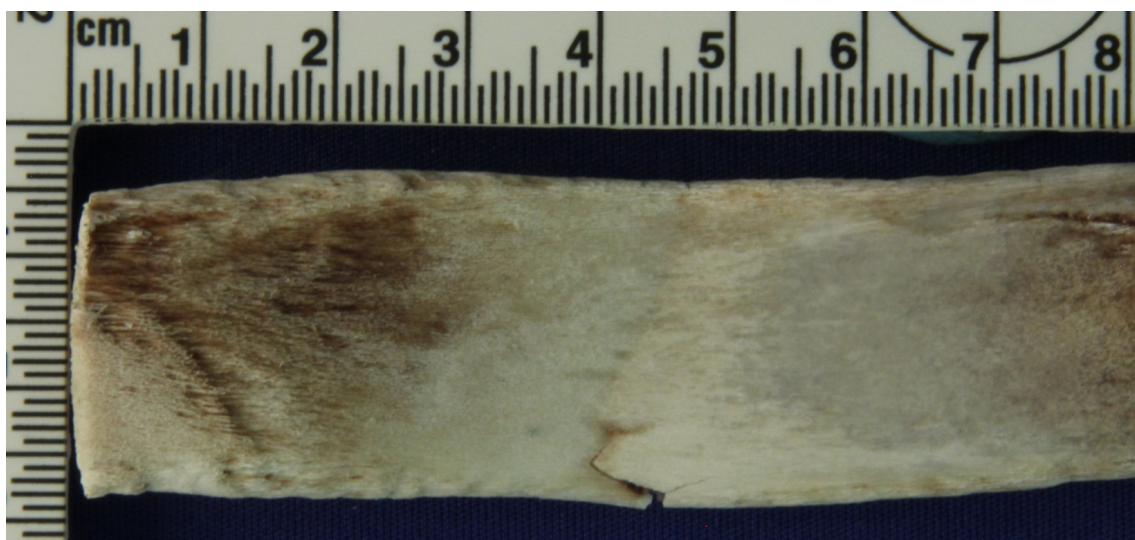


Figure 3.5a 2RLR3 exhibiting a greenstick fracture (Photo by K.A. Boyd)

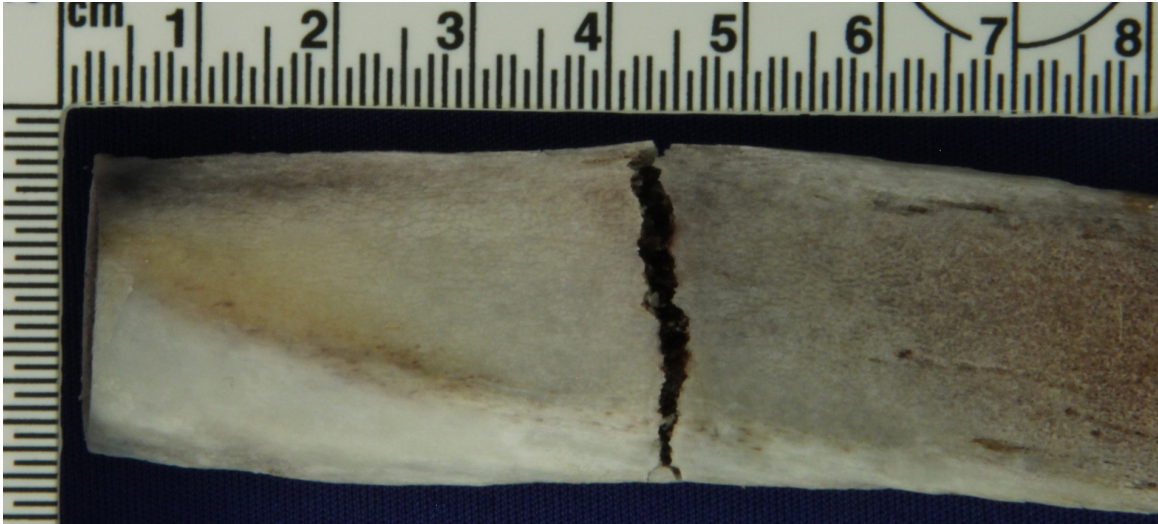


Figure 3.5b 2RLR3 exhibiting a greenstick fracture (Photo by K.A. Boyd)

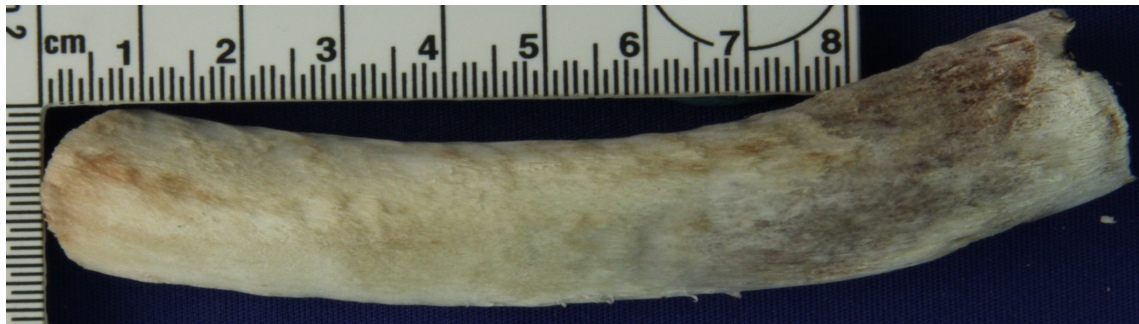


Figure 3.6 2RUR5 exhibiting no fracture (Photo by K.A. Boyd)

3.2 Force Determination

After all the rib samples were macerated and analyzed for their fracture type, their associated graphs were retrieved from the computer software. In this study, there was only an interest in the amount of force that was applied to the ribs, therefore the impact force graph was the only graph that was evaluated (Figure 3.7). The force at the direct moment of impact, when the hammer first met the rib samples, was determined to be the very first peak seen on the graph. The remaining peaks that were seen on the graph are caused by the oscillation of the arm of the machine and the load cell. The reason why there is a such a difference between the first few peaks and the peaks following is believed to be because the hammer would first strike the semi-fleshed portion on the bone, bounce back, and then fracture the bone the rest of the way though.

Although once believed to be a problem with this experiment, and that the force at the moment of impact should be taken from these higher peaks, the determination was kept the same as this experiment is trying to simulate blunt force trauma attacks on the rib cage where a human would have flesh overlying their ribs.

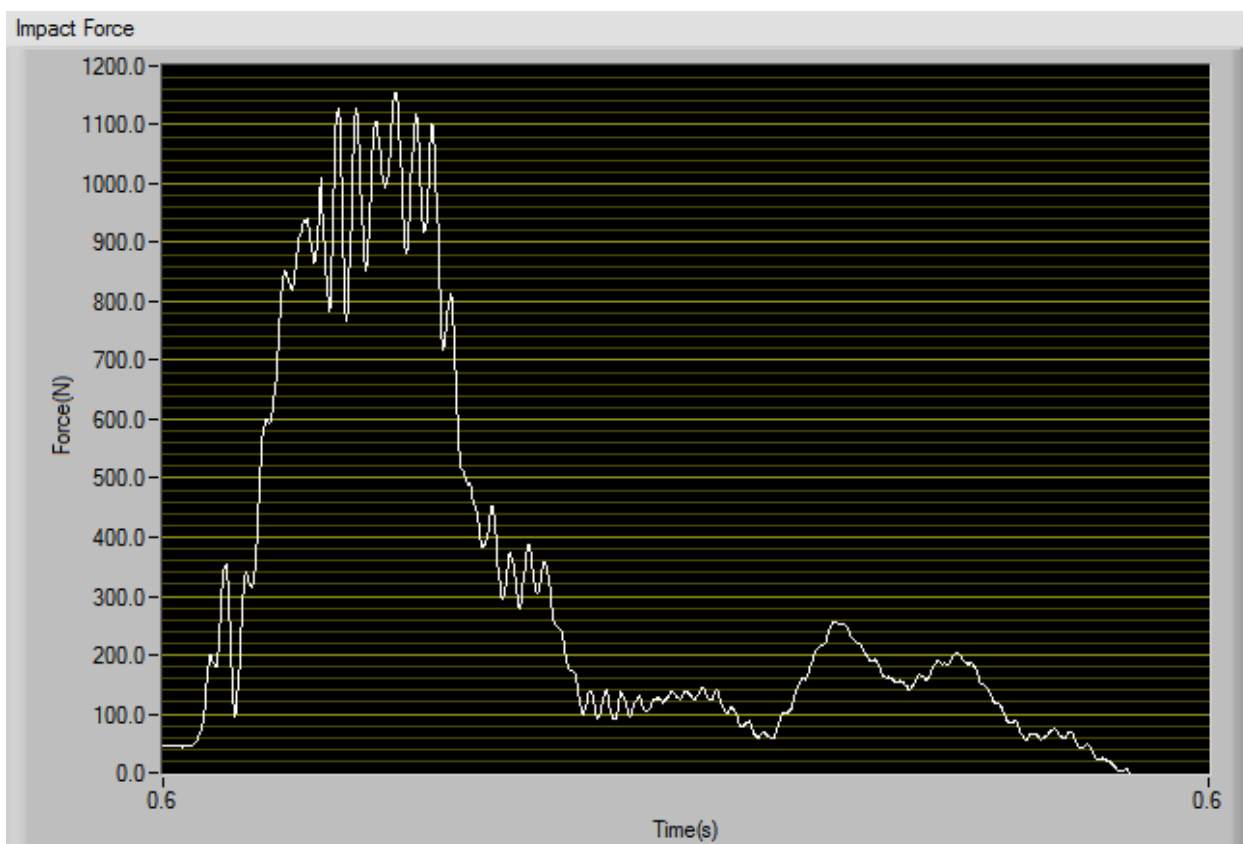


Figure 3.7 Graph generated by the impacting computer system for the force applied throughout the trial

3.3 Fracture and Force Association

After each of the fracture types were determined, and their associated forces were retrieved from the computer, they were paired side-by-side (Refer to Appendix I). This study was only interested in the force applied and its associated fracture type, so individual rib and rack numbers were overlooked. Table 3.1 lists the different fractures seen, the number of fractures obtained and their associates ranges, and the mean, standard deviation, and standard error of

those forces. These forces and their associated fractures types were plotted in a box and whisker plot to visualize the range and overlap of the fracture types (Figure 3.8).

Table 3.1 Fractures observed after impact and their associated ranges of force

Type of Fracture	# of Fractures	Range of Forces (N)	Mean of Forces (N)	Standard Deviation	Standard Error
Transverse	19	106.5- 696.3	356.9	139.8	32.1
Oblique	4	137.0 - 330.0	260.5	90.9	45.4
Greenstick	3	146.8 - 347.9	257.5	102.1	58.9
Spiral	2	406.4 - 604.2	505.3	139.9	98.9
Comminuted	3	361.1 - 204.1	383.9	192.3	111.0
No Fracture	5	115.8 - 367.2	229.0	110.4	49.4

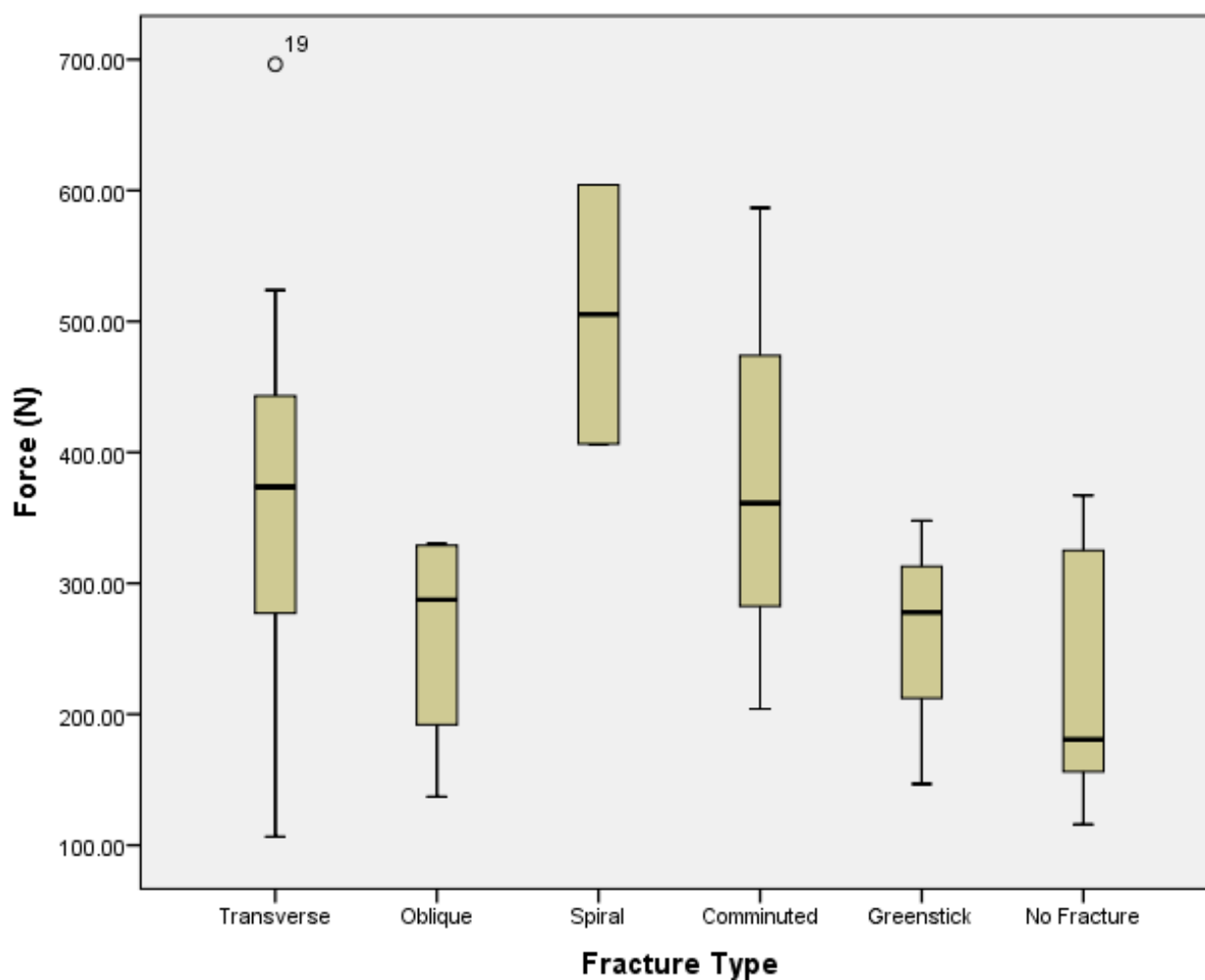


Figure 3.8 Box and whisker plot displaying the overlap between forces applied and their associated fracture types

3.4 Statistical Analysis

All statistics for this experiment were conducted in Microsoft® Excel (version 15.32). The first test that was performed was a series of Modified Thompson Tau test for outliers. This test measures the differences between the measured value and the mean of the fracture category. As seen in the box and whisker blot in Figure 3.8, there was one outlier in the transverse category, a value of 696.3N. This value was eliminated from the rest of the statistical tests as it may have happened by chance as it lies outside the body of the group. The test was run again, and there were no more remaining outliers.

A Kruskal-Wallis test was performed to investigate if the distribution of force was the same across the different fracture category types. A non-parametric ANOVA was used as normality cannot be assumed for such a small sample set. The test established that there were no significant differences, as the calculated K value (8.80) was less than the critical value (11.1).

Multiple Mann-Whitney U tests for unpaired, uneven variance data were conducted to compare the medians of the fracture categories two-by-two. These tests demonstrated that there were no differences between any of the fracture groups. Three more Mann-Whitney U tests were conducted to explore if there were any differences between the medians of left and right transverse fractures, and upper and lower rack transverse fractures, and fresh and thawed transverse fractures. Such tests also showed no significant differences. The results from these tests can be seen in Table 3.2.

Table 3.2 Table representing the results from multiple Mann-Whitney U tests

Categories of Comparison	U _{critical} Value Calculated	Significance Level	Significance Value
Transverse vs. Oblique	51	0.05	60
Transverse vs. Spiral	30	0.05	34
Transverse vs. Comminuted	31	0.05	47
Transverse vs. Greenstick	40	0.05	47
Transverse vs. No Fracture	69	0.05	72
Oblique vs. Spiral	8	0.02	8
Oblique vs. Comminuted	9	0.01	12
Oblique vs. Greenstick	7	0.1	12
No Fracture vs. Oblique	12	0.05	19
Comminuted vs. Spiral	5	0.2	6
No Fracture vs. Oblique	12	0.05	19
Comminuted vs. Spiral	5	0.2	6
No Fracture vs. Oblique	12	0.05	19
Comminuted vs. Spiral	5	0.2	6
Greenstick vs. Spiral	6	0.2	6
Transverse Fractures of Left Ribs vs. Transverse Fractures on Right Ribs	19	0.05	25
Transverse Fractures on Upper Ribs vs. Transverse Fractures on Lower Ribs	7	0.2	12
Transverse Fractures on Fresh Ribs vs. Transverse Fractures on Thawed Ribs	42	0.05	61

One T-test was also performed assuming normality between fractured and non-fractured ribs. This proved, again, that there were no significant differences between the forces applied to both groups. The t-value calculated was a value of 0.10, and the critical value at 5% was a value of 2.04.

CHAPTER 4: DISCUSSION

This study was conducted to try to replicate the results of a previous experiment by C. Holinier, however, there were many discrepancies between the two studies, the first being the sample size. This experiment subjected 36 individual juvenile rib bones to direct trauma, and the previous study had a sample size of 19 exhibiting the fractures observed in this experiment. This smaller sample size resulted in the previous study showing no comminuted fractures, and only one spiral fracture. The differences in fractures seen between the two experiments can be seen in Table 4.1. The statistics used in the previous study assumed normality and discovered significant differences between the force applied when comparing juvenile ribs that were struck and did not fracture to those of the transverse and oblique fracture groups. These results may have suffered from the low sample size, as this study used a slightly larger size and found no such significant differences.

Figure 4.1 Table comparing the different fractures seen between this study, and the study by C.Holinier

This Study		Previous Study	
Fracture Type	Times Observed	Fracture Type	Times Observed
Transverse	19	Transverse	8
Oblique	4	Oblique	4
Spiral	2	Spiral	1
Comminuted	3	Comminuted	-
Greenstick	3	Greenstick	3
No Fracture	5	No Fracture	3

Since the experiment done by Holinier was conducted, there has been calibration in the load cell of the impacting device, resulting in vast differences between the graphs produced. When examining the graphs, we can see that those produced in this study (Figure 3.7) account for more oscillation of the arm and the hammer than when compared to the previous study (Figure 4.1). We can also see that the first peaks, being the force at the moment of impact, are

very different from one another. This results in a large difference between the forces utilized between the two experiments. In the previous study, Holinier concluded that at least 700N was required to result in the fracturing of the rib bones, however, in this experiment a transverse fracture was observed at 106.5N. This difference may have occurred not only due to the calibration of the machine, but could also be caused by methodological differences between the experiment as well, such as letting pressure into the piston. A summary of the forces and fracture types of the previous experiment are shown in Table 4.2.

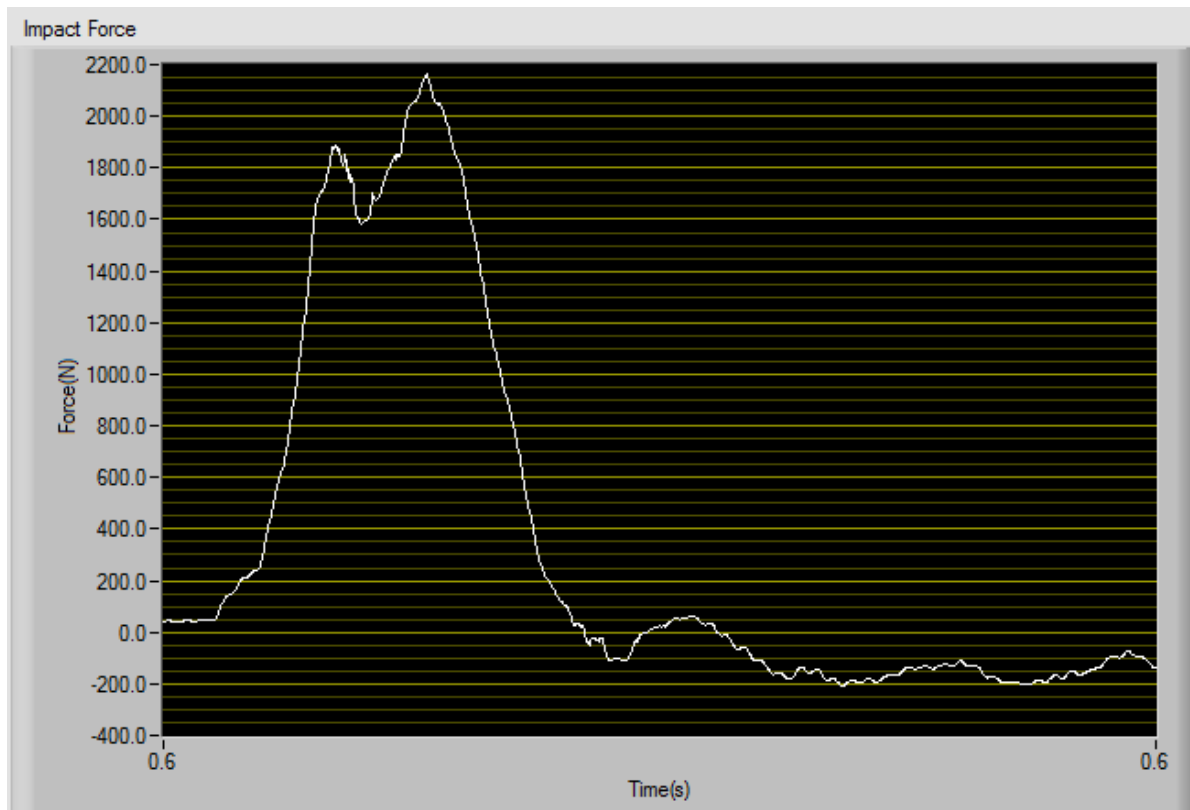


Figure 4.1 Graph generated by the impacting computer system for the force applied throughout the trial of C.Holinier's study

Table 4.2 Fractures observed after impact and their associated ranges of force of C.Holinier's study

Type of Fracture	# of Fractures	Range of Forces (N)	Mean of Forces (N)	Standard Deviation	Standard Error
Transverse	8	705.3 – 792.5	1277.5	580.3	205.2
Oblique	4	1125.6 – 1078.5	1479.1	435.8	217.9
Greenstick	3	651.2 – 796.3	1024.7	526.3	303.8
Spiral	1	1375.7	1375.7	-	-
Comminuted	0	-	-	-	-
No Fracture	3	685.9 – 214.6	458.7	236.1	136.3

To compare the results from both the experiments, a box and whisker plot was created from the data of Holinier (Figure 4.2). When compared to Figure 3.8 it is apparent that the relationships between force and fracture type in both experiments do not follow a distinct pattern. We can also visualize from the results of this experiment that there is a very large overlap of fracture types in the 300 – 400N range. This indicates that fracture types are not directly related to specific forces, or a range of specific forces in which one type will end and another will begin. We can see however, that if the means of the two experiments are plotted, the means between transverse, spiral, greenstick, and no fractures follow the same general pattern. No fractures happen at a lower force threshold than do any of the other fracture groups, which is to be expected. Spiral fractures, a more arguably “complicated” fracture type, happens when larger forces are applied followed by transverse, and then greenstick.

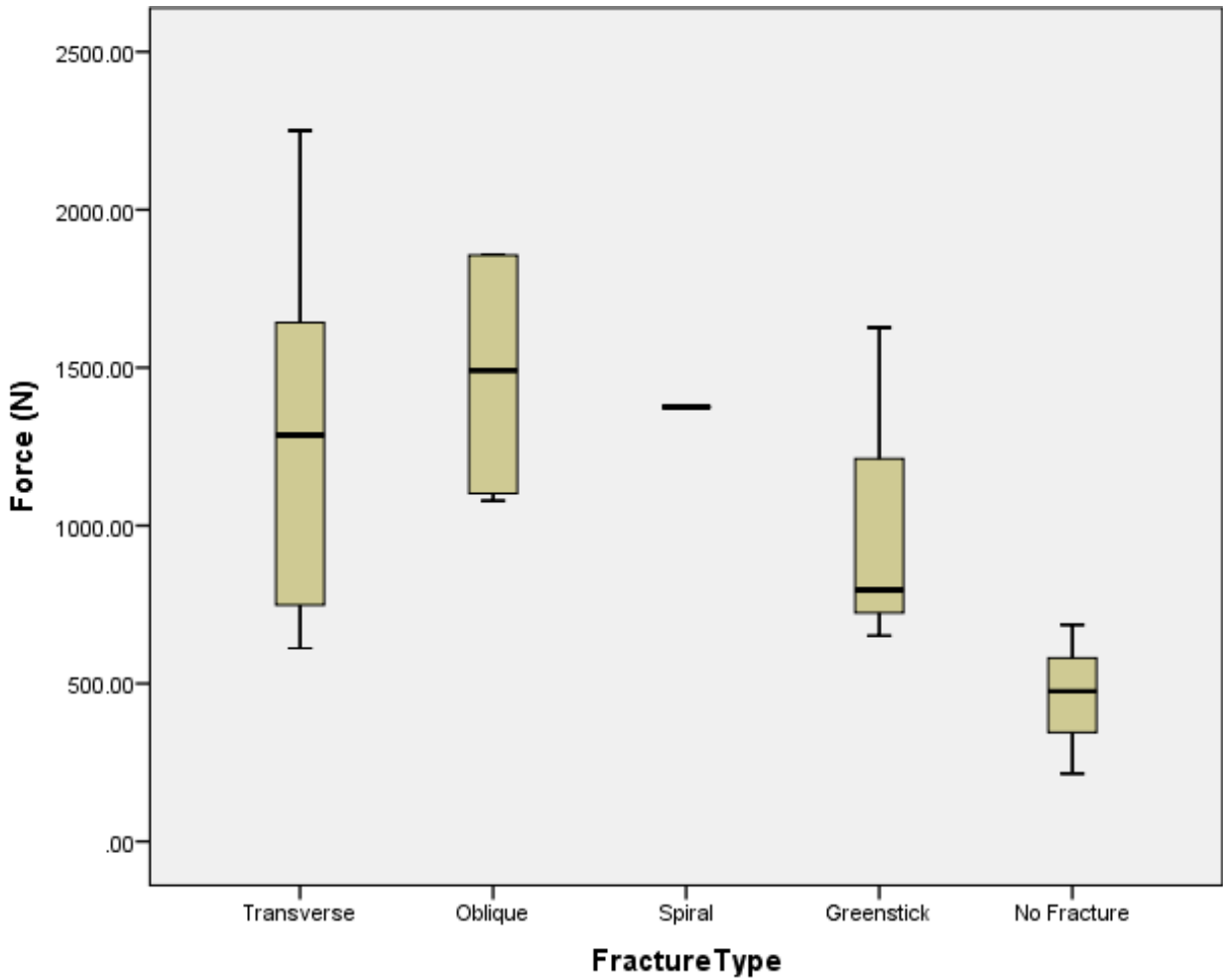


Figure 4.2 Box and whisker plot displaying the overlap between forces applied and their associated fracture types of C.Holinier's study

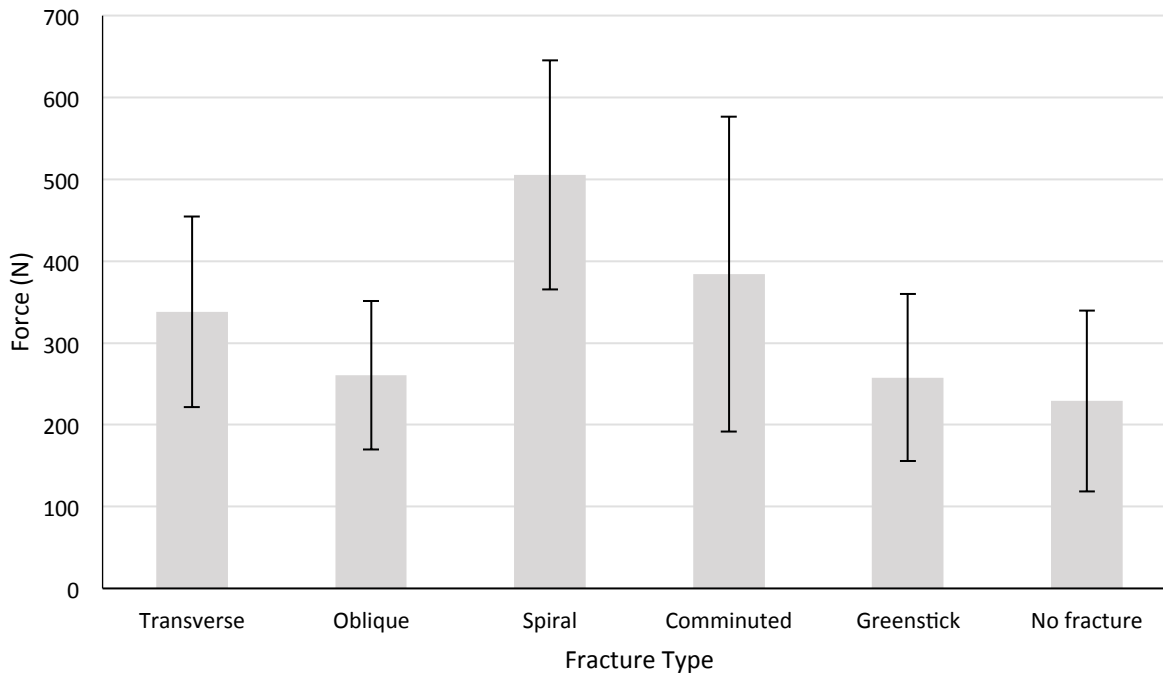


Figure 4.3 Graph representing the median distribution of the fracture types and their associated forces

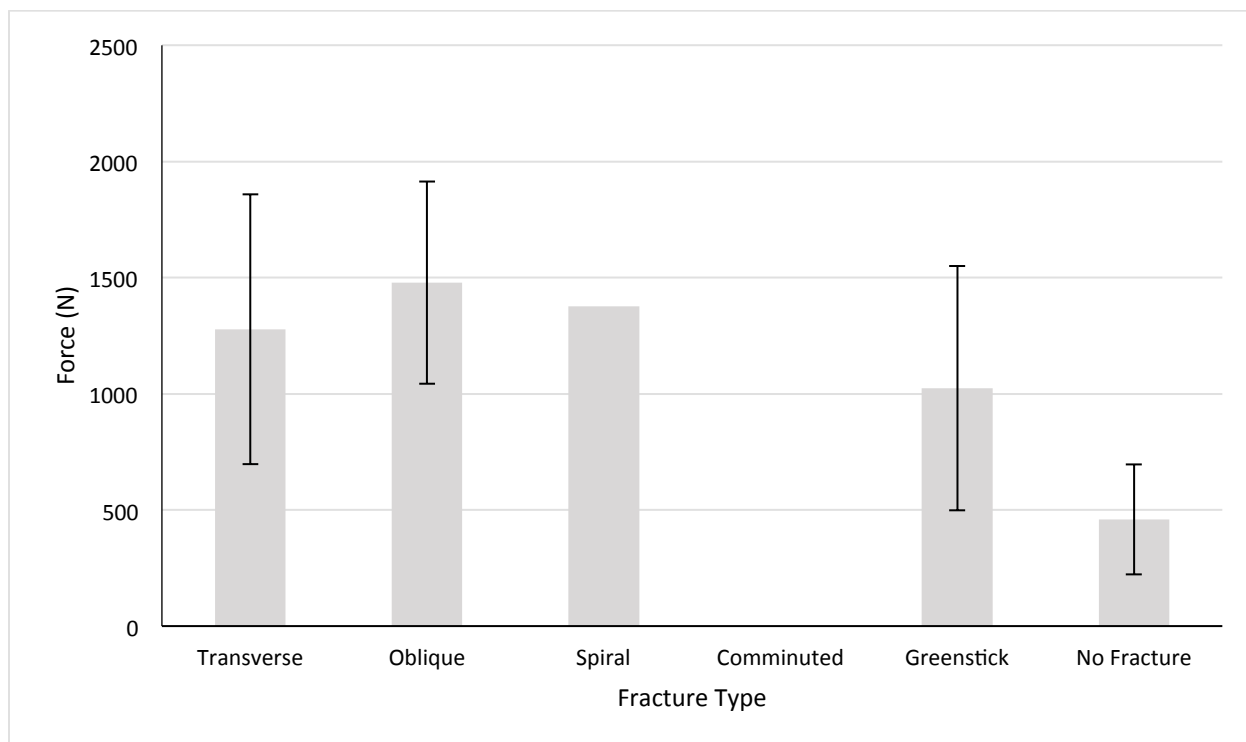


Figure 4.4 Graph representing the median distribution of the fracture types and their associated forces of C.Holinier's study

CHAPTER 5: CONCLUSIONS

5.1 Conclusions

Although we can visualize the beginnings of a relationship between force and fracture between the two studies, the results are still inconclusive. We can, however, conclude that transverse fractures were found to be the most prevalent type in both studies and there is a new minimum threshold of 106.5N resulting in fracture. Based on the results from this preliminary study (Figure 4.3), it is also suggested that more “complicated” fractures, such as those of spiral and comminuted, require more force to fracture than those of transverse and greenstick fractures, however this will need to be further investigated in future studies.

5.2 Limitations and Future Research

After there is full calibration of the machine, it is proposed that the experiment be conducted again and referred back to this study as well as the study of Holinier’s, to further investigate the relationship between force applied and fractures visualized on semi-fleshed articulated porcine ribs. It is suggested that such an experiment use a much larger sample size so all fracture types have the potential to be observed. One might also choose to utilize ballistic gelatin to help support the arching ribs when subjected to blows, preventing possible secondary fracturing from slippage through the metal plate more so than cardboard. Once successful, future experiments could be conducted to investigate relationships between force and fracture type on adult human ribs (with ethical agreements), and potentially investigate the differences between a force applied to a second rib and that same force applied to the seventh rib. Because the arm of the impactor can be interchanged, in the future one might want to investigate the experiment utilizing different blunt instruments (such as one with a larger surface area), or even sharp force trauma at different angles, and intercostally between bones.

APPENDIX I

RAW DATA

Table A: Each impacted rib number, it's associated fracture type and corresponding force (K.A. Boyd)

Rib	Force (N)	Transverse Fracture	Oblique Fracture	Greenstick Fracture	Spiral Fracture	Comminuted Fracture	No Fracture
1LUR2	200.2	X					
1LUR3	403.9	X					
1LUR4	523.9	X					
1LUR5	696.3	X					
1LUR6	604.2				X		
2LUR2	195.9	X					
2LUR3	274.9	X					
2LUR4	277.8			X			
2LUR5	359.9	X					
2LUR6	586.6					X	
2LUR7	451.7	X					
2LLR8	305.5	X					
2LLR9	300.9	X					
2LLR10	441.8	X					
2LLR11	327.8		X				
2LLR12	247.1		X				
2LLR13	180.8						X
2RLR3	146.8			X			
2RUR4	380.2	X					
2RUR5	367.2						X
2RUR6	457.4	X					
2RUR7	347.9			X			
2RLR8	325.1						X
2RLR9	418.0	X					
2RLR10	361.1					X	
2RLR11	279.4	X					
2RLR13	156.1						X
3LUR2	204.1					X	
3LUR4	330.0		X				
3LUR5	406.4				X		
3LUR6	444.3	X					
3LUR7	373.6	X					
3LLR8	166.1	X					
3LLR9	137.0		X				
3LLR10	115.8						X
3LLR11	106.5	X					

Table B: Each impacted rib number, it's associated fracture type and corresponding force (C. Holinier)

Rib	Force (N)	Transverse Fracture	Oblique Fracture	Greenstick Fracture	Spiral Fracture	Comminuted Fracture	No Fracture
1LUR1	796.3			X			
1LUR2	1382.1	X					
1LUR3	175.7						X
1LUR4	1264.1	X					
1LUR5	792.5	X					
1LUR6	214.6						X
1LLR7	1078.5		X				
1LLR8	1904.0	X					
1LLR9	1375.7				X		
1LLR11	1626.6			X			
1RUR1	612.0	X					
1RUR3	1309.3	X					
1RUR5	2250.8	X					
1RUR6	1856.2		X				
1RUR7	1856.2		X				
1RLR8	1125.6		X				
1RLR10	705.3	X					
1RLR12	651.2			X			
1RLR13	685.9						X

REFERENCES

- [1] Byers SN. Introduction to Forensic Anthropology, 2nd ed., Pearson Education, 2005.
- [2] Cohen H, Kugel C, May H, Medlej B, Stein D, Slon V, et al. The Impact Velocity and Bone Fracture Pattern: Forensic Perspective. *Forensic Sci Int* 2016 May;266:54-62.
- [3] Marinho L, Cardoso HFV. Comparing Known and Reconstructed Circumstances of Death Involving a Blunt Force Trauma Mechanism through a Retrospective Analysis of 21 Skeletonized Individuals. *J Forensic Sci* 2014 Nov;61(6):1416.
- [4] Reber SL, Simmons T. Interpreting Injury Mechanisms of Blunt Force Trauma from Butterfly Fracture Formation. *J Forensic Sci* 2015 Nov;60(6):1401-1411.
- [5] Aubert R, Pavier J, Eches N, Langlet A, Bailly P. On The Use of Hopkinson Bar-bending Apparatus to Study Soft Impact on Porcine Ribs. *Computer Methods in Biomechanics and Biomedical Engineering* 2012 Sept;15(S1):311-312.
- [6] Daegling DJ, Warren MW, Hotzman JL, Self CJ. Structural Analysis of Human Rib Fracture and Implications for Forensic Interpretation. *J Forensic Sci* Nov 2008;53(6):1301-1307.
- [7] Bolliger SA, Kneubuehl BP, Thali MJ, Eggert S, Siegenthaler L. Stabbing Energy and Force Required for Pocket-knives to Pierce Ribs. *Forensic Sci Med Pathol* 2016 Dec;12(4):394-398.
- [8] Galloway A, editor. Broken Bones: Anthropological Analysis of Blunt Force Trauma. Springfield, IL: Charles C Thomas, 1999.
- [9] Love JC, Symes S.A. Understanding Rib Fracture Patterns: Incomplete and Buckle Fractures. *J Forensic Sci* 2004 Nov;49(6):1-6.
- [10] Kanchan T, Menezes RG, Sirohi P. Penetrating Cardiac Injuries in Blunt Chest Wall Trauma. *J Forensic Legal Medicine* 2012 Aug;19(6):350-351.
- [11] Kimmerle EH, Baraybar JP. Skeletal Trauma: Identification of Injuries Resulting from Human Rights Abuse and Armed Conflict. Boca Raton, FL.: Taylor & Francis Group, 2008.
- [12] Barington K, Jensen HE. A Novel, Comprehensive and Reproducible Porcine Model for Determining the Timing of Bruises in Forensic Pathology. *Forensic Sci Med Pathol* 2016 Mar;12(1);58-67.
- [13] Hillier ML, Bell LS. Differentiating Human Bone from Animal Bone: A Review of Histological Methods. *J Forensic Sci* 2007 Mar;52(2):249-263.
- [14] Williams PL, Warwick R, Dyson M, Bannister LH, editors. Gray's Anatomy. New York, NY: Churchill Livingstone, 1989.

- [15] Martin RB, Burr DB, Sharkey NA, Fyhrie DP. Skeletal Tissue Mechanics. 2nd ed. New York, N.Y.: Springer Publishers, 2015.
- [16] Sommerfeldt DW, Rubin CT. Biology of Bone and How it Orchestrates the Form and Function of the Skeleton. Eur Spine J 2001 Oct;10(s02);S86-S95.
- [17] Horner JL. Premature Calcification of the Costal Cartilages: Its Frequent Association with Symptoms of Non-organic Origin. Am J Med Science 1949;218:186-193.
- [18] White TD, Folkens PA. Human Osteology. 3rd ed. Burlington, MA: Academic Press, 2011.
- [19] Kooi RJ, Fairgrieve SI. SEM and Stereomicroscopic Analysis of Cut Marks in Fresh and Burned Bone. J Forensic Sci 2013 Mar;58(2):425-428.
- [20] Lynn KS, Fairgrieve SI. Macroscopic Analysis of Axe and Hatchet Trauma in Fleshed and Defleshed Mammalian Long Bones. J Forensic Sci 2006 Jul;54(4):786-792.
- [21] Card A, Cross P, Moffatt C, Simmons T. The Effect of Clothing on the Rate of Decomposition and Diptera Colonization on *Sus scrofa* Carcasses. J Forensic Sci 2015 Jul;60(4):979-982.
- [22] Calce SE, Rogers TL. Taphonomic Changes to Blunt Force Trauma: A Preliminary Study. J Forensic Sci 2007 May;52(3):519-527.
- [23] Croft AM, Ferllini R. Macroscopic Characteristics of Screwdriver Trauma. J Forensic Sci 2007 Nov;52(6):1243-1251.
- [24] Hunt AC, Cowling RJ. Murder by Stabbing. Forensic Sci Int 1991 Dec;52(1):107-112.